

---

---

Submitted to the Proceedings of the US Community Study  
on the Future of Particle Physics (Snowmass 2021)

---

---

## Snowmass White Paper: Effective Field Theories for Dark Matter Phenomenology

---

Matthew Baumgart,<sup>a</sup> Fady Bishara,<sup>b</sup> Joachim Brod,<sup>c</sup> Timothy Cohen,<sup>d</sup> A. Liam Fitzpatrick,<sup>e</sup> Martin Gorbahn,<sup>f</sup> Ulserik Moldanazarova,<sup>g</sup> Matthew Reece,<sup>h</sup> Nicholas L. Rodd,<sup>i</sup> Mikhail P. Solon,<sup>j</sup> Robert Szafron,<sup>k</sup> Zhengkang Zhang,<sup>l</sup> Jure Zupan<sup>c</sup>

<sup>a</sup>*Department of Physics, Arizona State University, Tempe, AZ 85287, USA*

<sup>b</sup>*Deutsches Elektronen-Synchrotron DESY, Notkestr. 85, 22607 Hamburg, Germany*

<sup>c</sup>*Department of Physics, University of Cincinnati, Cincinnati, Ohio 45221, USA*

<sup>d</sup>*Institute for Fundamental Science, University of Oregon, Eugene, OR 97403, USA*

<sup>e</sup>*Department of Physics, Boston University, Boston, MA 02215, USA*

<sup>f</sup>*Department of Mathematical Sciences, University of Liverpool, Liverpool L69 3BX, United Kingdom*

<sup>g</sup>*Faculty of Physics and Technology, Karaganda Buketov University, 100028 Karaganda, Kazakhstan*

<sup>h</sup>*Department of Physics, Harvard University, Cambridge, MA, 02138, USA*

<sup>i</sup>*Theoretical Physics Department, CERN, 1 Esplanade des Particules, CH-1211 Geneva 23, Switzerland*

<sup>j</sup>*Mani L. Bhaumik Institute for Theoretical Physics, University of California at Los Angeles, Los Angeles, CA 90095, USA*

<sup>k</sup>*Department of Physics, Brookhaven National Laboratory, Upton, N.Y., 11973, USA*

<sup>l</sup>*Department of Physics, University of California, Santa Barbara, CA 93106, USA*

**ABSTRACT:** The quest to discover the nature of dark matter continues to drive many of the experimental and observational frontiers in particle physics, astronomy, and cosmology. While there are no definitive signatures to date, there exists a rich ecosystem of experiments searching for signals for a broad class of dark matter models, at different epochs of cosmic history, and through a variety of processes with different characteristic energy scales. Given the multitude of candidates and search strategies, effective field theory has been an important tool for parametrizing the possible interactions between dark matter and Standard Model probes, for quantifying and improving model-independent uncertainties, and for robust estimation of detection rates in the presence of large perturbative corrections. This white paper summarizes a wide range of effective field theory applications for connecting dark matter theories to experiments.

---

## Contents

<b>1</b>	<b>Executive Summary</b>	<b>2</b>
<b>2</b>	<b>Heavy DM: Direct Detection</b>	<b>2</b>
<b>3</b>	<b>Heavy DM: Indirect Detection</b>	<b>4</b>
<b>4</b>	<b>Heavy DM: Corrections to Sommerfeld Enhancement</b>	<b>7</b>
<b>5</b>	<b>Direct detection DM EFT for general mediators</b>	<b>9</b>
5.1	Three flavor DM EFT	10
5.2	EFT description of DM–nucleon interactions	13
5.3	Connecting to the UV	14
<b>6</b>	<b>EFTs for Table-top Direct Detection Experiments</b>	<b>15</b>
<b>7</b>	<b>Simplified mediator models for colliders</b>	<b>17</b>
<b>8</b>	<b>EFTs for DM self interactions</b>	<b>18</b>
<b>9</b>	<b>Conclusions</b>	<b>19</b>

---

## 1 Executive Summary

Effective Field Theory (EFT) techniques enable precise calculations of dark matter (DM) signals, and have already had a significant impact on the experimental searches in a number of cases, such as predicting DM annihilation rates relevant for imaging atmospheric Cherenkov telescopes, as well as DM scattering rates relevant for flagship direct detection experiments. The fixed order calculation of annihilation cross sections for heavy, TeV-scale, weakly-interacting massive particle (WIMP) dark matter into photons suffers from large Sudakov double logarithms. These were resummed using Soft Collinear Effective Theory to next-to-leading logarithmic (NLL) accuracy [1], reducing theoretical uncertainties from a factor of a few to the level of  $\sim 5\%$ . The improved predictions are being used by members of the HESS collaboration for interpreting their results [2], and are similarly incorporated into the ongoing analysis by the VERITAS telescope. The inclusion of the EFT effects is crucial: the leading order cross section for the Higgsino is just within the discovery reach of CTA [3] (assuming a canonical Milky Way dark matter distribution), and whether this well-motivated WIMP candidate can be discovered or excluded in the coming years hinges on where higher order corrections move the leading order prediction. In direct detection the use of EFTs allows for a model independent comparison of experiments. Because the momentum exchange in DM scattering on nuclei is small, the DM EFTs capture large classes of DM models, as long as mediators are heavier than a GeV. The direct detection EFT framework, either based on DM interactions with nucleons, or on DM couplings to quarks and gluons, was already adopted by a large number of experimental collaborations when interpreting their results [4–11].

This white paper also highlights a variety of other uses of EFT that further our understanding of DM phenomenology. High precision predictions for direct detection of heavy WIMPs were obtained through the use of a heavy particle EFT, while potential non-relativistic EFT was used to perform precise thermal relic abundance calculations for heavy WIMPs in the regime where Sommerfeld enhancements are important. Similarly, the implications of DM self-interactions for structure formation can be understood using nonrelativistic EFT. Additionally, new direct detection techniques for light DM with mass below a GeV rely on condensed matter effects that can be well described using EFTs. Finally, the collider searches for DM production have been interpreted using simplified models for the better part of the past decade.

Given these successes, it is clear that continued development of EFT tools for dark matter will be important for interpreting signals from current and future experiments, especially in the event of a discovery.

## 2 Heavy DM: Direct Detection

In a large class of models, the Standard Model is extended at low energies by one or a few particles transforming under definite representations of  $SU(2)_W \times U(1)_Y$  with masses much heavier than the electroweak scale,  $M \gg m_W$ . This is the case for a thermal relic electroweak

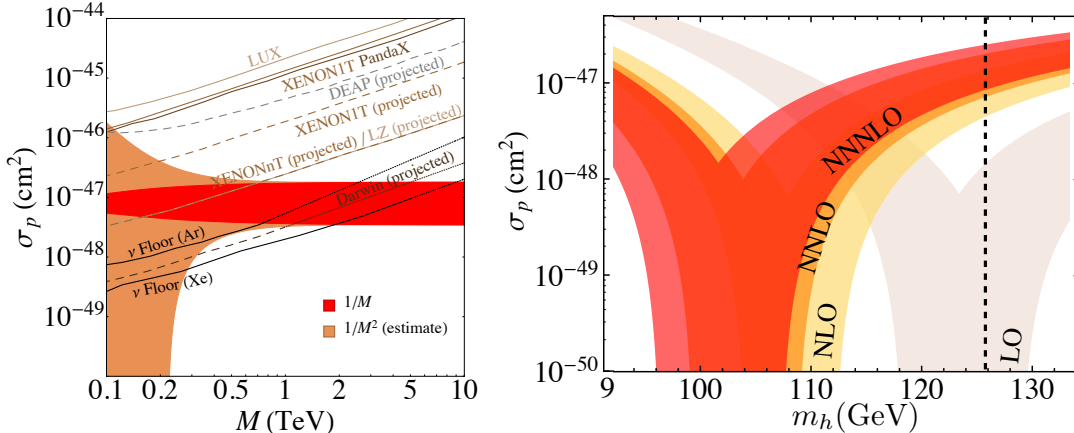


**Figure 1.** (Left) WIMP-proton scattering cross section as a function of the WIMP mass for a Majorana triplet. For  $M \gtrsim 700\text{GeV}$ , the prediction is given by the universal  $M \rightarrow \infty$  limit. The red band represents perturbative and hadronic input uncertainties, and includes sample model-dependent  $1/M$  corrections. The orange band estimates the impact of  $1/M^2$  corrections. Figure taken from Ref. [18]. (Right) The impact of perturbative QCD corrections on the universal cross section is illustrated as a function of the Higgs mass. Bands represent predictions including higher-order contributions (as labeled) to the running and matching calculations below the weak-scale. Figure taken from Ref. [16].

triplet (wino) or doublet (Higgsino), and is consistent with null results at the LHC and at direct detection experiments. For such models, we can apply a heavy particle formalism familiar from Heavy Quark Effective Theory [12–14] to develop a systematic framework for describing the interactions of such heavy WIMPs with Standard Model particles [15, 16].

Analogous to the case of heavy quarks, heavy WIMP symmetry emerges in the  $M \gg m_W$  limit. Spin-independent WIMP-nucleon scattering cross sections become universal for given WIMP electroweak quantum numbers, independent of the details of the UV completion. For example, the cross section does not depend on whether the DM is a scalar or fermion, or whether it is fundamental or composite in nature. This universality can be parametrized systematically in the  $1/M$  expansion:

$$\mathcal{L} = \bar{h}_v \left\{ i v \cdot D - \delta m - \frac{D_\perp^2}{2M} + c_H \frac{H^\dagger H}{M} + c_{W1} \frac{\sigma^{\mu\nu} W_{\mu\nu}}{M} + c_{W2} \frac{\epsilon^{\mu\nu\rho\sigma} \sigma_{\mu\nu} W_{\rho\sigma}}{M} + \dots \right\} h_v. \quad (2.1)$$

This Lagrangian specifies the interactions of  $h_v$ , a heavy multiplet of self-conjugate particles with arbitrary spin and transforming under irreducible representations of electroweak  $SU(2)_W \times U(1)_Y$ .<sup>1</sup> The coupling  $c_H$  gives the leading correction to the universal spin-independent cross-section in the heavy WIMP limit, and encodes ultraviolet physics, which can be determined by matching to a specified UV completion. The couplings  $c_{W1}$  and  $c_{W2}$  are the leading contributions to spin-dependent scattering at low-velocity.

<sup>1</sup>The timelike unit vector  $v^\mu$  defines the heavy WIMP velocity,  $D^\mu$  and  $W^{\mu\nu}$  are the usual covariant derivative and field strengths, and  $D_\perp^\mu = D^\mu - v^\mu v \cdot D$ . See, *e.g.*, Refs. [17, 18] for more details.

The simple universal heavy WIMP limit, obtained by taking  $M \rightarrow \infty$  in Eq. 2.1, was analyzed in Refs. [15, 16], and revealed that generic amplitude-level cancellations suppress the low-velocity WIMP-nucleon cross section by orders of magnitude compared to simple estimates. For instance, the cross section for the triplet was found to be  $\sim 10^{-47} \text{ cm}^2$ , and even smaller for the doublet. See Fig. 1. In the presence of such cancellations, formally subleading effects can become relevant. The impact of corrections from perturbative QCD is illustrated in the right panel of Fig. 1. The effect of the  $c_H$  parameter was explored in Refs. [18, 19], while the effect of multinucleon matrix elements was studied in Ref. [19].

While these small cross sections make heavy WIMPs more challenging to probe in direct detection experiments, the model-independence of the heavy WIMP limit provides a benchmark that can be precisely constrained by studying the underlying Standard Model interactions. This includes contributions from matching at the weak scale [17], from running between and matching at quark thresholds, and from evaluating hadronic matrix elements [20]. These calculations also involve a number of effective field theory methods such as those used in perturbative QCD and chiral perturbation theory. See Sec. 5 for further discussion.

Heavy particle methods have also been applied for studying the direct detection phenomenology for the case of an additional singlet (bino) [21], and have been extended and applied for resummation of large logarithms  $\sim \log M/m_W$  relevant for the case of indirect detection, as discussed in Sec. 3, as well as for analyzing corrections to Sommerfeld enhancement, as discussed in Sec. 4.

### 3 Heavy DM: Indirect Detection

In many dark matter scenarios, we can observe a flux of its annihilation or decay products from the ambient dark matter concentrations throughout the Universe. (See Ref. [22] for a recent overview of this “indirect detection of dark matter.”) As in Sec. 2, getting an observable signal is straightforwardly realized by augmenting the SM with additional particles charged under the electroweak  $SU(2)_W \times U(1)_Y$ . However, there are other possibilities, such as a coupling  $\mathcal{L} \supset \bar{\chi}\chi\bar{\psi}\psi$ , where  $\chi$  is the WIMP DM field that may be a SM singlet, and  $\psi$  is some SM field. The case of  $\psi = H$  is the so-called “Higgs portal,” and if  $\chi$  is itself a scalar, then the interaction even arises from a renormalizable operator [23] (*cf.* [24] for a current review).

In indirect detection, the presence of WIMP-WIMP interactions gives a richer structure to the heavy WIMP effective theory. If the DM is charged under the electroweak force (or another force with light mediators), then it is subject to a long-range potential. This can boost its annihilation rate via Sommerfeld enhancement, which is further detailed in Sec. 4. Additionally, the DM can bind into short-lived wimponium states, and for certain scenarios like the  $SU(2)_W$  quintuplet, the capture photons are nearly detectable with present experiments for certain masses [25]. Furthermore, the quintuplet offers an example of  $\mathcal{O}(10\%)$  modification to the annihilation rate to energetic photons from the additional wimponium channels [26].

For sufficiently heavy dark matter ( $M \gtrsim 1$  TeV) one must account for the presence of energies parametrically above the weak scale. Even in this regime though, the electroweak symmetry remains broken. Thus, even observables like the semi-inclusive annihilation rate to  $\gamma + X$  exhibit double-log-enhanced radiative corrections from Bloch-Nordsieck violation [27–29]. In the  $M_\chi \gg m_W$  regime, the event kinematics relevant for indirect detection resemble those of a collider experiment, but with showers of electroweak (rather than QCD) radiation accompanying the photon and recoil “jets.” The appropriate EFT to sum the large logs of the resulting scale hierarchies is soft-collinear effective theory (SCET) [30–33]. This was initially developed for WIMP annihilation in a series of papers studying  $SU(2)_W$  triplet or “wino” dark matter [1, 34–38], but one can go to other electroweak multiplets like higgsino [39, 40] or quintuplet [26] with similar machinery since many of the operator structures are the same. The main ingredients are the soft Wilson lines and collinear gauge fields whose interactions are highly constrained by the large gauge symmetry of SCET. The latter is expressed as

$$\mathcal{B}_{n\perp}^\mu(x) = \frac{1}{g} \left[ W_n^\dagger(x) iD_{n\perp}^\mu W_n(x) \right], \quad (3.1)$$

where  $W_n(x)$  is a collinear Wilson line given by

$$W_n(x) = \left[ \sum_{\text{perms}} \exp \left( -\frac{g}{\bar{n} \cdot \mathcal{P}} \bar{n} \cdot A_n(x) \right) \right]. \quad (3.2)$$

See *e.g.* Ref. [38] for a careful definition of these expressions. It is straightforward to include SCET fields for SM fermions and the Higgs, as well.

Simple electroweak WIMP scenarios yield multi-TeV photon line signals, making them natural targets for gamma-ray telescopes. Nonetheless, a benefit of developing the electroweak SCET is that it allows (along with standard QCD SCET) a first-principles resummation of the final state shower of radiation. Thus, the modification for different experimental scenarios is straightforward, as the same EFT can provide results for continuum photon,  $e^+/e^-$ , neutrino, or cosmic ray final states. Changing the initial dark matter process is simple, too, as one just requires a different high-scale annihilation or decay operator (like that of the Higgs portal) before passing to the SM SCET.

As stated above, a primary application of the heavy DM EFT framework is to indirect DM searches performed with terrestrial imaging atmospheric Cherenkov telescopes (IACTs). When a high-energy gamma-ray impacts the atmosphere, the charged particles present in the resulting shower produce Cherenkov radiation that can be detected on the Earth’s surface on sufficiently dark nights. Detecting this radiation, an IACT can reconstruct the incident photon with considerable angular and energy resolution. In exactly this manner, an IACT can search for the photons generated by heavy DM annihilating in the galactic center. The current generation of instruments searching for DM include MAGIC [41, 42], Veritas [43–45], and HESS [2, 46–48]. Observations of the center of the Milky Way – where the brightest signal from DM annihilation is expected – already place the thermal wino under tension. As explored in Ref. [2], to avoid these constraints one can exploit our uncertainty in the DM

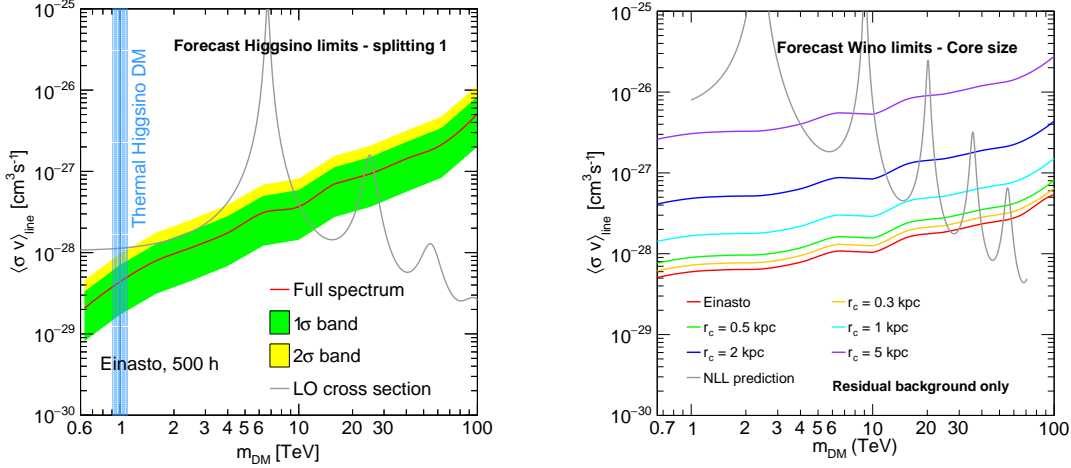


**Figure 2.** Results reproduced from Ref. [3] showing the sensitivity of CTA to Higgsino (left) and wino (right) DM annihilation in the galactic center. For the Higgsino, the result suggest that CTA could be sensitive to the cross-section predicted at the thermal mass  $\sim 1$  TeV. However, the theory prediction does not include the effects of the EFT of Heavy DM, which could easily shift the result in either direction by a factor of few, and provides a clear motivation for this work. For the wino, one sees that even with extremely conservative assumptions about the DM content of the inner galaxy, corresponding to a very large core size, the predicted cross section at the thermal mass of  $\sim 3$  TeV will be excluded (*cf.* at present this is not excluded by HESS [2]). We refer to Ref. [3] for additional details.

density in the inner part of the Galaxy. For instance, if instead of steadily increasing towards the galactic center the DM is cored within  $\sim 2$  kpc, then the predicted signal flux can be reduced below the current limits. The next generation IACT, the Cherenkov Telescope Array (CTA) [48–51], will be able to remove this caveat [3] (*cf.* Fig. 2). As shown in Ref. [3], CTA may also be able to probe the long sought after thermal Higgsino, a plot from that work demonstrating this is reproduced in Fig. 2. Yet this result did not draw on the EFT of Heavy DM, and whether this enhances or reduces the annihilation cross-section will determine the fate of this DM candidate in the coming years.

An interesting feature of the SCET used for indirect detection is the presence of two types of scale hierarchies. We straightforwardly have large logs of the form  $\log(M_\chi/m_W)$ . A key aspect of IACTs that further influences the required EFT calculations is the energy resolution. Thus, one also picks up large logs of the form  $\log(1 - z_{\text{cut}})$ , where  $z_{\text{cut}}$  is the energy fraction of the WIMP mass below which a photon cannot have come from a simple  $2 \rightarrow 2$  annihilation. For  $\mathcal{O}(\text{TeV})$  energy gamma-rays, existing instruments such as HESS can achieve  $\Delta E/E \sim 10\%$ , a value CTA will improve to  $\sim 5\%$  in the future. In either event, the resolution is insufficient to distinguish between the line spectrum – photons emerging from two-body final states, such as  $\gamma\gamma$  and  $\gamma Z$  – and those originating from so-called endpoint photons, which cannot be distinguished from the line photons given the finite resolution. This is why the

inclusion of endpoint photons is critical, and can impact the IACT sensitivities by an  $\mathcal{O}(1)$  factor [1, 38]. Of course it is also important to include photon contributions which can be distinguished from the line spectrum, broadly categorised as continuum photons. For example, these can emerge from the decay products of a  $W^+W^-$  final state, and can be incorporated using results provided in Refs. [52, 53]. We note that continuum photons play a key role in CTA’s sensitivity to the thermal Higgsino [3], as the telescope will have significantly enhanced sensitivity to lower energy gamma-rays than previous IACTs. In [40, 54–56], the authors used the numerical coincidence of  $(1 - z_{\text{cut}})$  and  $m_W/M_\chi$  over much of the range of current and upcoming experiments for a simple EFT treatment of the wino and Higgsino. Equating these scale hierarchies is not possible to do though, for the full dataset anticipated for the CTA experiment [3]. Thus, the Higgsino remains a compelling target for further theoretical study.

#### 4 Heavy DM: Corrections to Sommerfeld Enhancement

WIMP dark matter exhibits exciting phenomenology. As noted by Hisano et al. [57–59], the annihilation cross-section is substantially altered when the DM mass is above about 1 TeV due to the so-called Sommerfeld effect. In the non-relativistic regime, as the relative DM velocity approaches zero,  $v \rightarrow 0$ , the ladder diagrams formed by exchanges of weak gauge bosons between the DM particles are responsible for the enhanced corrections. Each loop is suppressed by a weak coupling constant  $\alpha_2$ , but it receives an enhancement by a factor  $M_\chi/m_W$ , where  $M_\chi$  is the DM mass. When  $\alpha_2 \times M_\chi/m_W \sim 1$ , the ladder diagrams must be summed to all orders in perturbation theory. This section describes an EFT formalism allowing us to compute DM annihilation cross-sections and relic density for models exhibiting Sommerfeld enhancement. The main advantage offered by the EFT formalism is systematic expansion and easiness of including higher-order corrections.

Potential non-relativistic EFT (PNRQED) is a natural framework for computing Sommerfeld factors [60–62]. PNRQED has been initially developed in the contexts of QED and QCD bound states and threshold problems [63–65]. It is obtained from the full theory after integrating out off-shell degrees of freedom. The counting parameter is given by velocity  $v \ll 1$ . The Lagrangian, written in terms of potential DM fields  $\chi_i$ , which form a multiplet under  $SU(2)_W$ , relevant for computations of annihilation cross section, is given by

$$\begin{aligned} \mathcal{L}_{\text{PNRDM}} = & \sum_i \chi_i^\dagger(x) \left( iD_i^0(t, \mathbf{0}) - \delta m_i + \frac{\partial^2}{2M_\chi} \right) \chi_i(x) \\ & - \sum_{\{i,j\},\{k,l\}} \int d^3\mathbf{r} V_{(ij),(kl)}(r) \chi_k^\dagger(t, \mathbf{x}) \chi_l^\dagger(t, \mathbf{x} + \mathbf{r}) \chi_i(t, \mathbf{x}) \chi_j(t, \mathbf{x} + \mathbf{r}). \end{aligned} \quad (4.1)$$

The mass splitting between the multiplet members, which has a substantial impact on phenomenology [66], is denoted by  $\delta m_i$  and  $V_{(ij),(kl)}(r)$  are the potentials. At the leading order,  $V_{(ij),(kl)}(r)$  is a combination of Coulomb terms due to photon exchange and Yukawa potentials arising from massive gauge bosons. For example, for DM forming a Majorana  $SU(2)_W$  triplet,



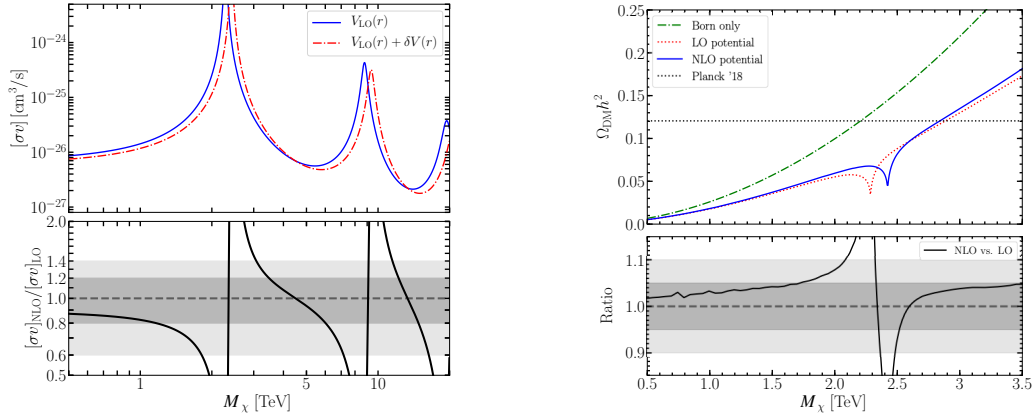


**Figure 3.** On the left: The annihilation rate  $\chi^0\chi^0 \rightarrow \gamma + X$ , computed with the LO (blue) and the NLO (red) potential as a function of DM mass. The ratio NLO/LO is shown in the lower panel with gray bands indicating the range where the correction stays below 20% and 40%. On the right: The relic abundance as a function of DM mass computed with Born cross sections (green), including LO (red) and NLO (blue) Sommerfeld enhancement. The horizontal line corresponds to the observed relic abundance. The lower panel illustrates the ratio of the NLO to LO Sommerfeld-corrected cross section. Plots reproduced from [67, 68].

we decompose the two-particle states into states with definite total angular momentum and spin, and find that the potential for the charge-neutral sector for the  $S$  wave spin-singlet  $^1S_0$  and triplet  $^3S_1$  configurations reads

$$V^{Q=0}(r)(^1S_0) = \begin{pmatrix} 0 & -\sqrt{2}\alpha_2 \frac{e^{-m_W r}}{r} \\ -\sqrt{2}\alpha_2 \frac{e^{-m_W r}}{r} & -\frac{\alpha}{r} - \alpha_2 c_W^2 \frac{e^{-m_Z r}}{r} \end{pmatrix}, \quad (4.2)$$

$$V^{Q=0}(r)(^3S_1) = \begin{pmatrix} 0 & 0 \\ 0 & -\frac{\alpha}{r} - \alpha_2 c_W^2 \frac{e^{-m_Z r}}{r} \end{pmatrix}. \quad (4.3)$$

The precise predictions for DM annihilation rates and relic abundance require inclusion of the next-to-leading order (NLO) potentials [67–69], especially near the location of the resonance. These corrections come from integrating out regions with soft momentum scaling. Often, the corrections affect the asymptotic behavior of the potentials. For example, massless fermions generate long-distance contributions, which dominate the behavior for large  $r$ . In the  $\chi^0\chi^0 \rightarrow \chi^+\chi^-$  channel, at the LO, only short-range Yukawa-type potential appears, but the NLO corrections change the asymptotic behavior to power-like  $\delta V(r) \sim 1/r^5$  behavior.

The  $\mathcal{L}_{\text{PNRDM}}$  describes the dynamics of the heavy particles. To describe annihilation, which is a short-distance process, it must be supplemented by higher-dimensional operators  $\delta\mathcal{L}_{\text{ann}}$  [60–62], whose Wilson coefficient are determined by matching the four-fermion operators on the full theory amplitude for  $\chi_i\chi_j \rightarrow \chi_l\chi_k$ .

The next step is to compute the co-annihilation cross-sections as functions of relative

velocity by taking relevant matrix elements of  $\delta\mathcal{L}_{\text{ann}}$ . The resulting expression combines Wilson coefficients and Sommerfeld factors for individual channels. The Sommerfeld factors are evaluated by solving the Schrödinger equation and are given by the incoming DM particles' scattering wave-functions evaluated at the relative distance equal to zero. In practice, the solution is performed numerically, as the analytical solutions of the Schrödinger equation with Yukawa potential are not known.

From here, determining the DM abundance requires the computation of the thermally averaged cross-section  $\langle\sigma_{\text{eff}}v\rangle$  for all possible co-annihilation channels. To compute the thermal relic DM abundance we solve the Boltzmann equation

$$\frac{dn(t)}{dt} + 3H(t)n(t) = -\langle\sigma_{\text{eff}}v\rangle(n^2(t) - n_{\text{eq}}^2(t)), \quad (4.4)$$

where  $n(t)$  is the total number density,  $H(t)$  is the Hubble rate and the  $n_{\text{eq}}(t)$  is the total equilibrium number density. Computing the present-day yield, we can obtain the relic density. The measured value of the DM abundance  $\Omega_{\text{DM}}h^2 = 0.1205$  is reproduced in a simple Wino model for  $M_\chi = 2.886$  TeV using LO potential and  $M_\chi = 2.842$  TeV for NLO potential, see the right plot in Fig. 3. A 2% shift is typical size for electroweak corrections away for the resonance region. The effect is more prominent for models where the location of the resonance plays a significant role. The resonance is achieved for  $M_\chi = 2.282$  TeV ( $M_\chi = 2.419$  TeV) for the LO (NLO) potential.

As the DM velocity is now much smaller than during the freeze-out, the NLO corrections are more pertinent for the present-day annihilation rate, shown in the left plot in Fig. 3, as a function of DM mass. The NLO corrections exceed 20% for a wide range of phenomenologically viable DM masses. Therefore, it is of paramount importance that NLO potential is included on a par with the resummation of soft and collinear effects.

The described non-relativistic EFT formalism can be applied to arbitrary models of heavy DM interacting with much lighter bosons. The NLO corrections to the non-relativistic potential can be found directly from [68] for  $SU(2)_W$ . They are also implemented in the code `DMγSpec` [56], which allows computing DM annihilation spectra  $\chi\chi \rightarrow \gamma + X$  that additionally include resummation of large electroweak corrections [1, 36, 38, 40, 54, 55, 70], see Sec. 3.

## 5 Direct detection DM EFT for general mediators

For a large class of DM models, the physics of direct detection experiments, where DM scatters on nuclei, can be described using effective field theories [15, 16, 18, 20, 21, 71–97]. The reason is that the momentum transfer  $q$  for DM scattering on a nucleus is small, typically less than 200 MeV, so that the effect of forces mediated by particles heavier than this scale can be described by an EFT. Furthermore, the interactions between the DM and the nucleus can be organized via a power counting parameter  $q/\Lambda_\chi$  where  $q$  is the momentum transfer and  $\Lambda_\chi$  is the chiral symmetry breaking scale, so that the interactions are organized by their chiral dimension [98, 99].

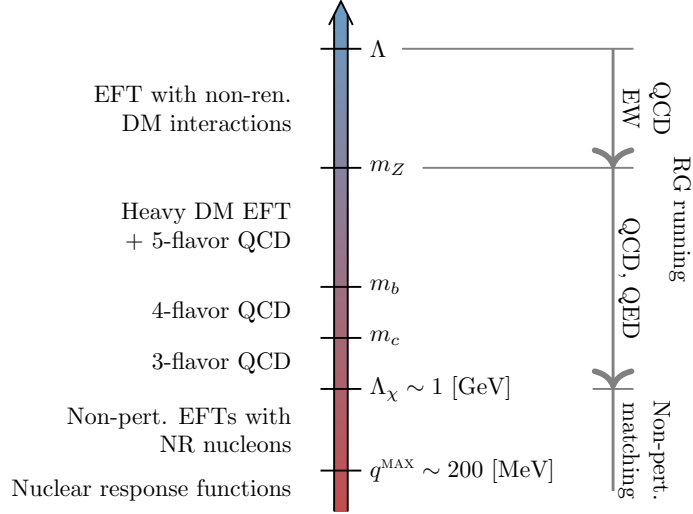


**Figure 4.** The tower of EFTs linking the UV scale  $\Lambda$  to the scale of interactions between the nucleons and the DM. Plot reproduced from [100].

The construction of DM EFTs for DM scattering on nuclei has two goals. The first goal is to compare the results of direct detection experiments that use different target materials in a model-independent way. To achieve this, a DM EFT valid at a scale  $\mu \simeq 2$  GeV can be constructed. The second goal is to connect the results of the direct detection experiments to the physics at much higher scales: indirect DM searches, DM production at the LHC, and ultimately to the full UV theory of DM. In this case one can construct a tower of EFTs, see Fig. 4.

At low energies, the interactions of DM with the SM can be parametrized in two different ways. The first is in terms of an EFT where DM interacts with quarks, gluons, and photons (three-flavor DM EFT at  $\mu \simeq 2$  GeV [88]). The second option is the Galilean invariant EFT, or NR EFT, in which DM interacts with non-relativistic neutrons and protons [77, 78, 80]. Here, we focus first on the three-flavor DM EFT, while parametrization using NR EFT is discussed in Sec. 5.2.

### 5.1 Three flavor DM EFT

In the three-flavor DM EFT, the operators are organized in terms of operator dimensions so that the effective Lagrangian takes the form

$$\mathcal{L}_{\text{DMEFT}} = \sum_{d,a} \frac{C_a^{(d)}}{\Lambda^{d-4}} Q_a^{(d)}, \quad (5.1)$$

where  $C_a^{(d)}$  are dimensionless Wilson coefficients, and  $\Lambda$  is the typical scale of the UV theory for DM. The sum is over different operators,  $Q_a$ , of dimension  $d$ . An example of a  $d = 6$  operator for fermionic DM is  $(\bar{\chi}\gamma^\mu\chi)(\bar{q}\gamma_\mu q)$  for a vectorial interaction; a typical  $d = 7$  operator

is  $(\bar{\chi}\chi)G_{\mu\nu}^a G^{a\mu\nu}$  for a scalar interaction. The full basis of operators for scalar and fermion DM of up to and including dimension seven can be found in [93], while the basis for vector DM was given in [96]. The expansion in (5.1) assumes that there is a mass gap between the DM candidate and the mediators,  $m_\chi \ll \Lambda$ . If that is not the case, i.e., if the mediators have a mass comparable to that of the DM or are even lighter, the appropriate description is in terms of the Heavy DM EFT discussed in Sec. 2.

The DM EFT (or Heavy DM EFT) facilitates a model-independent comparison of direct detection experiments, which is best done as follows: the Wilson coefficients  $\mathcal{C}_a^{(d)}$  in three-flavor DM EFT can be treated as unknown and are freely varied in a fit. The DM scattering rates for different targets are obtained by first matching onto NR EFT, or more generally the chiral EFT [85, 87, 101]. The leading-order expressions are given in Ref. [88], but sub-leading contributions, such as the effect of two-body currents, can also be included [95, 101, 102]. They are then used to obtain the DM–nucleus scattering cross sections. For both steps one can use public codes, `DirectDM` [90] in combination with `DMFormFactor` [80], or `ChiralEFT4DM` [95]. For a general Dirac fermion DM, 25 independent combinations of Wilson coefficients  $\mathcal{C}_a^{(d)}$  would be varied in three-flavor EFT fits when considering operators up to dimension-seven (excluding  $d = 7$  operators with derivatives) and at leading order in the chiral expansion. While this is still a rather large set of parameters, the benefit is that this approach captures all UV models for DM of a given spin with mediators heavier than a few hundred MeV.

One could instead entertain comparisons of direct detection experiments by only allowing for a subset of Wilson coefficients to be non-zero. The two well-known limits already widely used are spin-independent and spin-dependent scattering, but one can extend this to other well motivated benchmark choices, some of which we list below:

**Spin-independent (SI) scattering.** The operators  $(\bar{\chi}\gamma^\mu\chi)(\bar{q}\gamma_\mu q)$ ,  $(\bar{\chi}\chi)(\bar{q}q)$ ,  $(\bar{\chi}\chi)(GG)$  all lead to spin-independent scattering. That is, at leading order in chiral expansion they give rise to NR EFT operators,  $L_{\text{NR}} = c_1^N \mathbb{1}_\chi \otimes \mathbb{1}_N$ , where  $\mathbb{1}_\chi(\mathbb{1}_N)$  are the number operators for DM (nucleons) and the sum over  $N = p, n$  is implied. For the comparison of direct detection experiments under the assumption of SI scattering it suffices, therefore, to vary the SI couplings of DM to protons and neutrons,  $c_1^{p,n}$ .

**Spin-dependent (SD) scattering.** In the NR limit there are two types of interactions between the DM spin,  $\vec{S}_\chi$ , and nucleon spin,  $\vec{S}_N$ ,  $L_{\text{NR}} = c_4^N \vec{S}_\chi \cdot \vec{S}_N + c_6^N (\vec{S}_\chi \cdot \vec{q})(\vec{S}_N \cdot \vec{q})/m_N^2$ . Conventionally, in the comparisons of direct detection experiments under the assumption of pure SD scattering, the  $c_6^N$  are set to zero, which corresponds to taking just the tensor operator  $(\bar{\chi}\sigma_{\mu\nu}\chi)(\bar{q}\sigma^{\mu\nu}q)$  in the three-flavor DM EFT to be nonzero. An alternative limit is to assume that only the axial–axial operator  $(\bar{\chi}\gamma_\mu\gamma_5\chi)(\bar{q}\gamma^\mu\gamma_5q)$  is relevant, in which case both  $c_4^N$  and  $c_6^N$  are generated, the latter with a parametric size  $c_6^N \sim m_N^2/(m_\pi^2 + \vec{q}^2)$ , but numerically only important for scattering of DM on heavier nuclei.

**Gluophilic pseudoscalar mediator.** A pseudoscalar mediator such as an axion-like particle (ALP) that couples to a fermionic DM and to the SM through the QCD anomaly (for

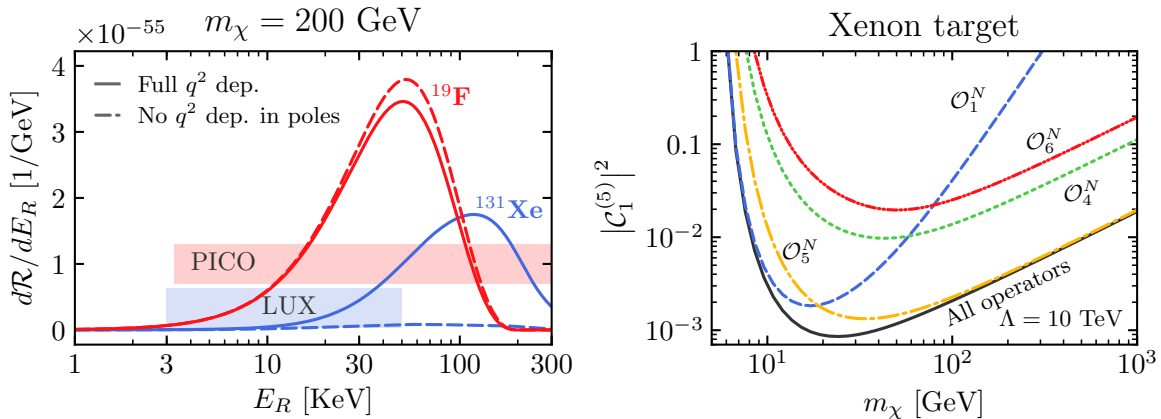


**Figure 5.** *Left panel:* recoil energy dependence for the ‘pseudoscalar mediator’ benchmark. The dashed lines show the artificial limit of neglecting terms proportional to  $\bar{q}^2$ . The shaded bands show the sensitivity windows for PICO and LUX. *Right panel:* contributions to the exclusion curve from the various NR operators in the case of magnetic dipole moment DM scattering on xenon. Plots reproduced from [100].

simple realizations in 2HDM + singlet scenarios see, *e.g.*, [103]) would give rise to the three flavor operator  $\bar{\chi}i\gamma_5\chi G^{a\mu\nu}\tilde{G}_{\mu\nu}^a$ . This results in a SD scattering with rather complicated  $\bar{q}^2$  pole structure in the  $c_6^N$  coefficient, after matching onto NR EFT. The scattering rates on light nuclei, such as fluorine, and heavier nuclei, such as Xenon, can then be quite different from the conventional SD scattering benchmark discussed above, see Fig. 5 (left).

**Magnetic dipole DM.** If DM mediators are heavy and charged under the electroweak SM gauge group, but do not directly couple to quarks, the leading interaction between fermionic Dark Matter and the SM will be via the DM magnetic dipole moment,  $\mathcal{Q}_1^{(5)} = \frac{e}{8\pi^2} \bar{\chi}\sigma^{\mu\nu}\chi F_{\mu\nu}$ . This induces  $c_1^N, c_4^N, c_5^N, c_6^N$  NR EFT coefficients that give different relative contributions when scattering on heavy or light nuclear targets, and on whether DM is lighter or heavier. An example for xenon target is shown in the right panel of Fig. 5.

**Vector mediator for Majorana DM.** For Majorana DM there are four relevant operators in the three-flavor DM EFT:  $(\bar{\chi}\gamma_\mu\gamma_5\chi)(\bar{q}\gamma^\mu q)$ ,  $(\bar{\chi}\gamma_\mu\gamma_5\chi)(\bar{q}\gamma^\mu\gamma_5 q)$ , where  $q = u, d$  (the  $(\bar{\chi}\gamma_\mu\chi)$  currents vanish for Majorana fermions). The simplest UV realization for these a tree-level exchange of a heavy  $Z'$ , in which case electroweak gauge invariance requires that the four Wilson coefficients in three-flavor DM EFT are expressed in terms of just three operators,  $(\bar{\chi}\gamma_\mu\gamma_5\chi)(\bar{Q}_L\gamma^\mu Q_L)$ ,  $(\bar{\chi}\gamma_\mu\gamma_5\chi)(\bar{u}_R\gamma^\mu u_R)$ , and  $(\bar{\chi}\gamma_\mu\gamma_5\chi)(\bar{d}_R\gamma^\mu d_R)$ , with coefficients that can be parametrized as  $(g'^2/\Lambda^2)\{\cos\theta, \sin\theta\cos\phi, \sin\theta\sin\phi\}$ , respectively [104]. This means that one cannot simultaneously suppress  $A\otimes V$  and  $A\otimes A$  operators for both up and down quarks. The effect is especially important for heavy nuclei, where  $A\otimes V$  and  $A\otimes A$  operators can give contributions of similar sizes to the direct-detection cross sections. An example for scattering

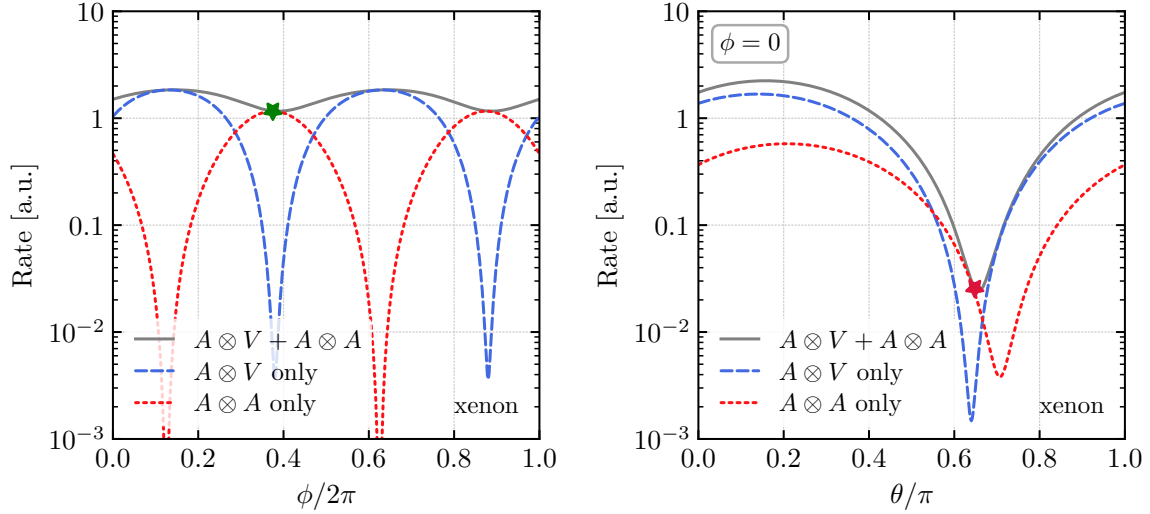


**Figure 6.** Relative event rate in direct detection on a Xenon target for  $\tan \theta = 2/(\sin \phi + \cos \phi)$  (left panel) and  $\phi = \pi$  (right panel) for Majorana DM with a vector mediator. The stars denote potentially anomaly free models, which are studied in more detail in Ref. [104]. Plots reproduced from [104].

on xenon is shown in Fig. 6, with the two panels showing the dependence on parameters  $\phi$  and  $\theta$ , when varying one and fixing the other.

## 5.2 EFT description of DM–nucleon interactions

Instead of three flavor DM EFT, in which DM couples to quarks and gluons, one can also use NR-EFT [77, 78, 80], in which DM couples to nonrelativistic nucleons, in order to parametrize the unknown interactions of DM. That is, instead of performing the series of matchings shown in Fig. 4, starting with the three flavor DM EFT, and then nonperturbatively matching onto NR-EFT, followed by the calculation of nuclear response to DM scattering, one can just as easily use NR-EFT directly as the starting point, given that the DM interactions are not known yet. To leading order in the chiral expansion, DM only couples to single nucleon currents, and thus the effective DM interactions take the form [77, 78, 80]

$$\mathcal{L}_{\text{NR}} = \sum_a c_a^N(q) \mathcal{O}_a^N, \quad (5.2)$$

where the interaction operators  $\mathcal{O}_a^N$  involve the non-relativistic DM and nucleons, with the latter only entering in the form of single nucleon currents. The UV physics is encoded in the coefficients  $c_a^N$  where different UV models may match onto the same NR operators. For instance, both vector and scalar mediators give rise to an operator  $\mathbb{1}_\chi \otimes \mathbb{1}_N$ , where  $\mathbb{1}_\chi$  ( $\mathbb{1}_N$ ) are the number operators for DM (nucleons). A single UV interaction may also result in several nonzero  $c_a^N(q)$ .

One main benefit of using NR-EFT is that the interactions are written trivially for any value of DM spin. Moreover, because short distance scales below the nucleon radius are integrated out, many different UV models can be subsumed into a smaller set of effective couplings; for instance, several operators in the three-flavor DM EFT all lead to the spin-independent operator in the NR EFT. Furthermore, the nucleon-level interactions are more directly connected to nuclear response functions, which are determined by the internal structure of atomic nuclei. The nuclear response functions can be calculated once and for all, and thus also the cross sections for DM scattering on nuclei, as long as the coefficients  $c_a^N(q)$  are given. The main drawback is that the cutoff of the NR-EFT is reduced compared to the three-flavor DM EFT, or more complete UV models, and therefore it has a smaller regime of validity; moreover, the use of three flavor DM EFT makes the connection with the UV models of DM more immediate. The coefficients  $c_a^N(q)$  are  $q$  dependent, and in a strict EFT approach would be treated as a series expansion in powers of  $q$  divided by the cutoff. However, light fields such as the photon and pion that are below the cutoff, and should in principle be included in the effective theory, might nevertheless be ‘integrated out’ for convenience, in which case they can generate additional poles in the  $c_a^N(q)$  coefficients. Taking  $c_a^N(q)$  to be constant in interpreting the data (see, *e.g.*, [105–111]) then captures only a subset of all possible DM models. Alternatively, one can limit the discussion to just a subset of possible DM interactions, for instance only to interactions that do not depend on nuclear spin, but gain in describing all possible choices for DM spin.

### 5.3 Connecting to the UV

When connecting the results of direct detection experiments to the UV theory of DM several different scales enter: the DM mass,  $m_\chi$ , the scale of the DM-SM mediators,  $\Lambda$ , and, finally, the standard model (SM) scales – the masses of the SM particles and the scale of strong interactions,  $\Lambda_{\text{QCD}}$ . The hierarchy between these scales determines which EFTs constitute the tower that connects the direct detection and UV scales, see, *e.g.*, Fig. 4. The main goal is to provide leading-order predictions for direct detection rates for any choice of a UV theory, which requires constructing the EFTs for each self-consistent ordering of the EFT scales, as well as for various DM spins and electroweak quantum numbers.

We emphasize that in particular cases electroweak corrections need to be included to obtain the leading predictions, since they mix operators with very different non-relativistic limits. Fig. 7 shows the effect of electroweak corrections for two examples of Dirac fermion DM interactions of the type  $(\bar{\chi}\gamma_\mu\chi)(\bar{u}_i\gamma^\mu\gamma_5u_i + \bar{d}_i\gamma^\mu\gamma_5d_i)$ , with  $i = 1, 2, 3$  the generational index, and with DM an electroweak singlet (triplet) in Fig. 7 left (right). Fig. 7 left assumes flavor universality. Without electroweak radiative corrections DM scattering is due to an interaction term  $(\bar{\chi}\gamma_\mu\chi)(\bar{u}\gamma^\mu\gamma_5u + \bar{d}\gamma^\mu\gamma_5d)$  with very small, both spin and velocity suppressed, nuclear matrix elements (dashed lines). At one loop there is a top yukawa induced  $V \otimes V$  operator proportional to  $(\alpha_t/(4\pi)) \log(M_W/\Lambda)$  that results in much larger coherently enhanced rates and more stringent exclusions (solid lines). Fig. 7 left assumes the dimension 6 operator involves only couplings to the third generation in the UV. For  $\Lambda = 1 \text{ TeV}$  the radiatively

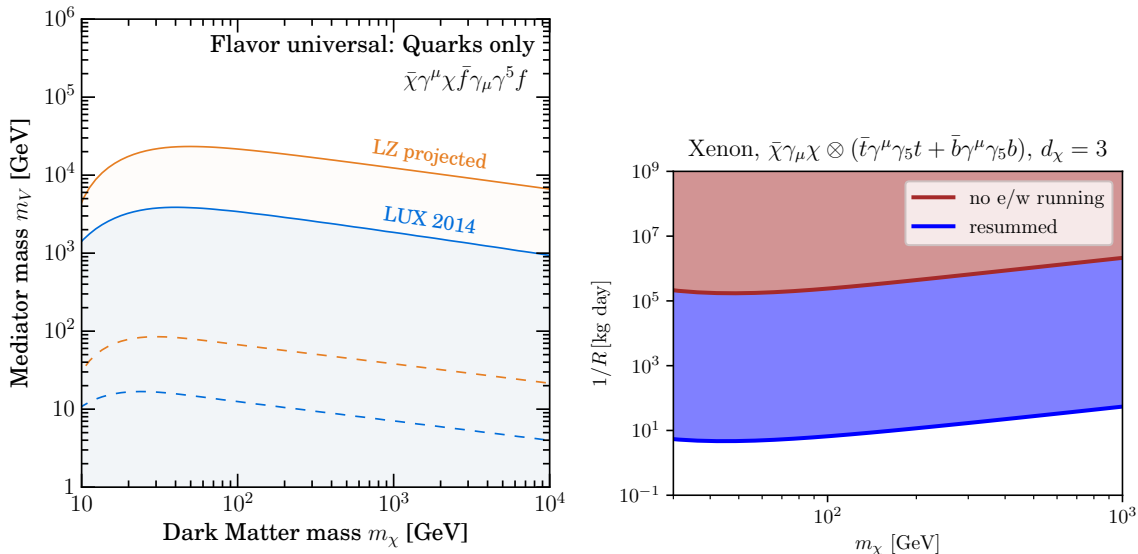


**Figure 7.** Left: exclusions on DM mass for  $V \otimes A$  flavor universal  $\mathcal{O}(1)$  couplings to quarks for electroweak singlet Dirac fermion DM with dashed (solid) lines denoting exclusions without (with) inclusion of RG running. Right: predicted inverse rates for  $V \otimes A$  operators with couplings of electroweak triplet Dirac fermion DM to only third generation quarks where resummed RGEs are included (blue) or not (red). Plots reproduced from [89, 100].

induced corrections from higher dimension  $V \otimes A$  operator (blue) dominate by orders of magnitude compared to the electroweak renormalizable interactions that enter at two loops (red). Another illustrative example is electroweak triplet Dirac fermion DM with  $V \otimes A$  couplings to only the first generation of quarks. The RG flow generates the  $(\bar{\chi}\gamma_\mu\chi)(\bar{u}\gamma^\mu\gamma_5 u + \bar{d}\gamma^\mu\gamma_5 d)$  interactions that is enhanced by a *quadratic* logarithm  $\alpha_2^2/(4\pi)^2 \log^2(M_W/\Lambda)$ . That is, even though the effect arises at *second order* in operator mixing, the induced interaction gives the leading contribution to the scattering rate, larger than the original interaction by up to two orders of magnitude for scattering on heavy nuclei. While the effect would correspond to a two-loop correction in the “full theory”, the DM EFT automatically captures the leading-logarithmic part of it. A full discussion of all radiative corrections relevant for dimension-six interactions can be found in Ref. [100], see also Refs. [89, 91, 92, 112, 113].

## 6 EFTs for Table-top Direct Detection Experiments

Theoretical developments over the last decade have led to the realization that compelling models of DM may have masses well below the weak scale. Meanwhile, new table-top experiments targeting sub-GeV DM have been proposed and are under active development. Sensitivity to lighter DM requires both sensors with better energy resolution and qualitatively new ideas. Conventional searches based on nuclear recoils have limitations: once the mass of DM drops below that of the nucleus, the detection rate suffers from a kinematic



suppression. We know, however, that condensed matter systems host a range of small-gap excitations as well as gapless modes. They could enable efficient extraction of a large fraction of the DM’s kinetic energy even for DM much lighter than a GeV. See Ref. [114] for a recent review.

To bridge the condensed matter knowledge with DM detection ideas, calculations of material responses to DM interactions are needed, with a combination of analytic and numerical tools. In particular, EFT methods [115–120] are useful both for classifying DM interactions and identifying condensed matter systems and excitations with favorable response to each type of interaction, and for generally formulating calculations of DM detection rates to facilitate automation.

For example, electronic excitations in noble gas atoms and dielectric crystals can arise from DM-electron scattering or absorption of bosonic DM coupling to electrons, and are being actively searched for by several experimental collaborations, including XENON, SuperCDMS, SENSEI, DAMIC, EDELWEISS. For general DM models, we can utilize the EFT framework to make signal rate predictions in terms of a set of atomic/crystal response functions, which are calculated from matrix elements of NR effective operators for DM-electron interactions in the detector medium [117, 119, 120].

Direct detection can also proceed via production of collective excitations, such as phonons and magnons, in the primary DM scattering process. To calculate the rate from the set of NR effective operators (which form an expanded basis compared to the nuclear recoil case due to in-medium violation of Galilean invariance), we match them onto lattice degrees of freedom in the long wavelength limit, which include the number of  $\psi = p, n, e$  particles contained in each ion  $\langle N_\psi \rangle$ , their total spin  $\langle \mathbf{S}_\psi \rangle$ , orbital angular momentum  $\langle \mathbf{L}_\psi \rangle$  and tensorial spin-orbit coupling  $\langle \mathbf{L}_\psi \otimes \mathbf{S}_\psi \rangle$ . These four types of couplings are referred to as crystal responses, as they play an analogous role as nuclear response functions in the nuclear recoil EFT calculation. In the present case, these crystal responses enter the effective DM-lattice scattering potential, which is then quantized in terms of phonon or magnon modes. In the simplest cases, phonon excitations in a crystal proceed through  $\langle N_\psi \rangle$  [121–124] and magnon excitations proceed through  $\langle \mathbf{S}_e \rangle$  [125]. More generally, all four types of crystal responses can lead to phonon excitations in appropriately chosen targets, while both  $\langle \mathbf{S}_e \rangle$  and  $\langle \mathbf{L}_e \rangle$  can lead to magnon excitations.

This EFT framework for direct detection with collective excitations [118] has been implemented in a publicly available code PhonoDark [126], and provides theory support for the ongoing experimental effort on phonon readout via *e.g.* transition edge sensors in SPICE and HeRALD experiments [127]. It also sets up the stage for investigating other condensed matter systems to identify new detector targets, a direction we look forward to further pursuing in the future.

## 7 Simplified mediator models for colliders

We have not yet observed any signals of DM being produced at colliders. This could be due to DM being too weakly coupled to the SM or simply being too heavy. An interesting intermediate possibility is that DM is light enough to be produced at colliders, and has appreciable couplings to other states, but interacts with the visible sector only through mediators that are too heavy to be efficiently produced at the LHC. At low energies the DM interactions with the SM are then described by an appropriate EFT, where the heavy mediators between DM and the SM particles were integrated out. Such an EFT based approach is ideal for interpreting the results of DM scattering in direct detection experiments, in which the typical momentum exchange,  $q \lesssim 200$  MeV, is much less than the mediator mass in most DM models, see Sec. 5.

The use of such EFTs to describe the results of LHC searches for DM, on the other hand, is more suspect. The cross sections for DM production, induced by non-renormalizable operators, grow with energy. For example, a dimension-6 operator of the form  $(\bar{\chi}\gamma_\mu\chi)(\bar{q}\gamma^\mu q)$  is suppressed by  $1/\Lambda^2$ , where  $\Lambda$  is the NP scale. This then results in a DM production cross section that scales as  $\sigma \sim E^2/\Lambda^4$ , and thus a large part of experimental sensitivity at the LHC may well come from collision energies at which the EFT description breaks down. There is an interplay between how precisely the SM backgrounds are predicted and how much statistics the LHC experiments are able to gather, which then translates to bounds on  $\Lambda$ . Typically, these are not stringent enough to be in the EFT regime,  $\Lambda \gg E$ , except for a small region of parameter space where the mediator couplings are close to the nonperturbative limit. In a very large part of the relevant parameter space the mediators are instead light enough to be produced directly in  $pp$  collisions. It is thus much better to interpret the bounds on DM production at the LHC by constructing the EFTs where the SM is supplemented by both DM and the mediator – the so called “simplified models” [128–155]. The complete UV models of DM would contain further degrees of freedom, which are assumed to be heavy and integrated out.

The simplified models differ in the assumed spin and the SM gauge quantum numbers of the mediators. The most commonly considered simplified models are: the  $s$ -channel color-neutral vector or axial-vector mediator, the  $s$ -channel color-neutral scalar or pseudo-scalar mediator, and the  $t$ -channel color-triplet scalar or pseudo-scalar mediator [103, 145, 156–160]. It is important that the simplified models satisfy the SM gauge invariance in order not to arrive at spurious violations of unitarity in predictions for the cross sections. In some cases this requires introducing more states beyond just the mediator. For instance, for a pseudo-scalar mediator the community has endorsed the use of the simplest such choice: a two Higgs doublet with a singlet pseudo-scalar that couples to DM (the 2HDM+ $a$  model). In some instances it is also important to include electroweak radiative corrections when comparing the results of LHC searches with direct detection results, see Section 5.3.

Phenomenologically, there are several qualitative differences between the use of EFTs with and without mediators. Importantly, in the EFTs that include the mediators one is able to capture the constraints on the UV models of DM which are placed by searches for

mediators when these decay not to DM pairs but to other visible final states such as muons, electrons, jets, etc. In many cases these are the most stringent constraints on the simplified models that are otherwise missed in EFTs constructed by integrating out the mediators. In simplified models one still needs to make a number of choices for mediator couplings when interpreting the data (for instance, the flavor composition of couplings to quarks, whether or not the mediators couple to leptons, etc). While simplified models assume minimal field content, the freedom of choice for various couplings results in simplified models that are not so very simple and thus capture many of the most important features of the full UV models.

## 8 EFTs for DM self interactions

The Sommerfeld effect discussed in Sec. 4 can be relevant not only for dark matter annihilation, but also for dark matter scattering. Self-interacting dark matter has received a great deal of attention, in part due to its possible role in explaining the structure of galaxies on smaller scales; see [161] for an extensive review. It is well-known that relatively long-range forces, like Yukawa interactions mediated by a scalar or vector much lighter than the dark matter particle itself, can lead to enhanced scattering at low velocity, which may be understood by resumming ladder diagrams in QFT or by solving a non-relativistic Schrödinger problem. For various studies of the Sommerfeld effect for Yukawa interactions, see [162–167].

Because self-interactions can involve important non-relativistic effects, it is appropriate to match the underlying relativistic QFT of self-interacting dark matter onto a non-relativistic effective theory [13, 168]. This was first done for dark matter self-interactions in [169], using the same classification of operators [170] that underlies the EFT for DM–nucleus scattering discussed above. In the initial work along these lines, a detailed matching to the underlying QFT was not carried out, which effectively meant that computations were being done in potentials with additional (possibly strong) short-range scattering—an artifact of improper matching, rather than actual physics. In particular, different early studies reached different conclusions about whether dark matter scattering via the exchange of a pseudoscalar mediator exhibits Sommerfeld enhancement. Because such models can arise in natural ways (*e.g.*, with the mediator being a pseudo-Nambu-Goldstone boson), it is important to assess whether the Sommerfeld enhancement exists in this case and what the correct velocity-dependence of pseudoscalar-mediated DM scattering is.

Recently, these calculations have been clarified via a simple new procedure for correctly matching the predictions of relativistic QFT onto a non-relativistic Schrödinger problem. The key idea is illustrated in Fig. 8 (reproduced from Ref. [171]). The nonrelativistic effective theory is expected to break down at high momentum, and hence at short distances. This makes possible a matching procedure where the non-relativistic EFT is defined only outside a finite radius, *e.g.*,  $a \sim 1/m_\chi$ . The tree-level QFT cross section at low velocities is matched to the leading order Born approximation in non-relativistic QM. This matching can be achieved by imposing a boundary condition on the wavefunction at the radius  $a$ . Subsequently, the full nonperturbative solution in the non-relativistic EFT can be achieved simply by solving

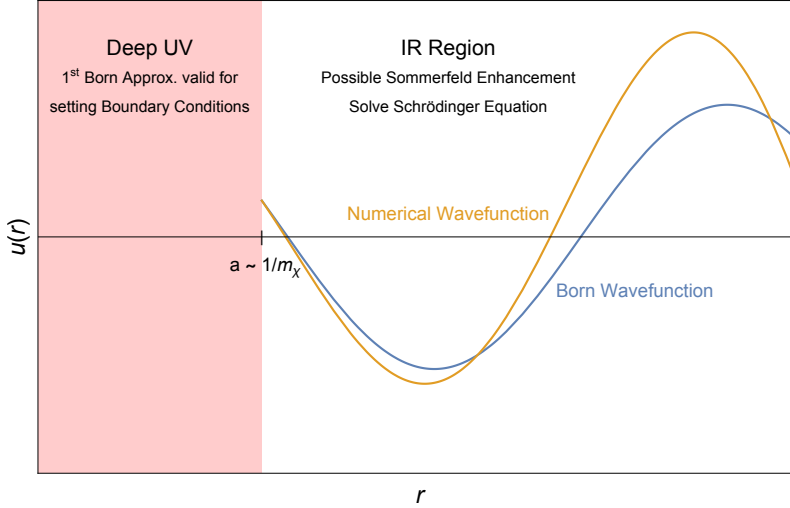


**Figure 8.** Illustration of the matching procedure from QFT to a non-relativistic Schrödinger problem with boundary at small radius, reproduced from Ref. [171].

the Schrödinger equation at  $r > a$  with the correct boundary condition. The boundary condition essentially arises from evaluating the Born approximation to the wave function in the region  $r < a$ , which turns out to be finite for the effective potentials arising from tree-level QFT (see also [172]). With this matching procedure, one can explicitly check that dark matter scattering via a pseudoscalar mediator does not exhibit any Sommerfeld enhancement: the tree-level QFT calculation is a good approximation to the solution to the Schrödinger equation. This can also be understood by a study of the behavior of ladder diagrams, and reinforces earlier claims of no Sommerfeld enhancement for pseudoscalar mediators [173]. The new matching procedure can be applied to a variety of other problems, including dark matter annihilation. Its extension beyond tree level would be an interesting target of further study.

## 9 Conclusions

The landscape of phenomenologically viable dark matter models is vast. It is often the case that there can be a large separation of scales involved in relating such models to observables, implying that effective field theory techniques could be relevant. This could be due to the parameters of the theory, *e.g.* if the dark matter mass is much larger than the electroweak scale. It could also be the result of the kinematics relevant to the observable of interest, *e.g.* direct detection experiments are looking for non-relativistic collisions between dark matter and nucleons.

The EFT paradigm provides a systematic approach for computing observables as a low energy expansion. When viewed from the bottom up, it is a tool for characterizing the allowed interactions among the propagating degrees of freedom. EFT is also useful from the top down: in the presence of a large separation of scales, one can integrate out the

heavy physics to derive an EFT Lagrangian which often simplifies calculations and can often facilitate more sophisticated calculations that could not have been done using the UV theory along. In particular, one can utilize renormalization group evolution to resum large logarithms that appear when one calculates using the UV theory directly. Both of these themes play a prominent roles in the work described above.

Clearly, the importance of applying EFT techniques to the DM question has led to significant improvements in our ability to calculate processes that are relevant across a huge range of experiments and observations. It additionally allows us to systematically classify the possible types of interactions the DM can have with the Standard Model, so that we can be systematic in our experimental approach. Further refinements and new ideas for EFT applications in DM are an active area of research. EFT will continue to play a pivotal role in the search for an experimental signature of DM.

**Acknowledgements.** M.B. is supported by the DOE (HEP) Award DE-SC0019470. A.L.F. is supported in part by the US Department of Energy Office of Science under Award Number DE-SC0015845. J.Z. acknowledges support in part by the DOE grant de-sc0011784 and NSF OAC-2103889. M.R. is supported by the DOE Grant DE-SC0013607, the NASA Grant 80NSSC20K0506, and the Alfred P. Sloan Foundation Grant No. G-2019-12504. R.S. acknowledge support by the United States Department of Energy under Grant Contract No. DE-SC0012704. T.C. is supported by the U.S. Department of Energy, under grant number DE-SC0011640. Z.Z. is supported by the U.S. Department of Energy under the grant DE-SC0011702. M.P.S. is grateful to the Mani L. Bhaumik Institute for Theoretical Physics for support.

## References

- [1] M. Baumgart, T. Cohen, E. Moulin, I. Moutl, L. Rinchiuso, N. L. Rodd et al., *Precision Photon Spectra for Wino Annihilation*, *JHEP* **01** (2019) 036, [[1808.08956](#)].
- [2] L. Rinchiuso, N. L. Rodd, I. Moutl, E. Moulin, M. Baumgart, T. Cohen et al., *Hunting for Heavy Winos in the Galactic Center*, *Phys. Rev. D* **98** (2018) 123014, [[1808.04388](#)].
- [3] L. Rinchiuso, O. Macias, E. Moulin, N. L. Rodd and T. R. Slatyer, *Prospects for detecting heavy WIMP dark matter with the Cherenkov Telescope Array: The Wino and Higgsino*, *Phys. Rev. D* **103** (2021) 023011, [[2008.00692](#)].
- [4] XENON collaboration, E. Aprile et al., *Effective field theory search for high-energy nuclear recoils using the XENON100 dark matter detector*, *Phys. Rev. D* **96** (2017) 042004, [[1705.02614](#)].
- [5] PANDAX-II collaboration, J. Xia et al., *PandaX-II Constraints on Spin-Dependent WIMP-Nucleon Effective Interactions*, *Phys. Lett. B* **792** (2019) 193–198, [[1807.01936](#)].
- [6] CRESST collaboration, G. Angloher et al., *Limits on Dark Matter Effective Field Theory Parameters with CRESST-II*, *Eur. Phys. J. C* **79** (2019) 43, [[1809.03753](#)].

- [7] DARKSIDE-50 collaboration, P. Agnes et al., *Effective field theory interactions for liquid argon target in DarkSide-50 experiment*, *Phys. Rev. D* **101** (2020) 062002, [[2002.07794](#)].
- [8] CDEX collaboration, Y. Wang et al., *First experimental constraints on WIMP couplings in the effective field theory framework from CDEX*, *Sci. China Phys. Mech. Astron.* **64** (2021) 281011, [[2007.15555](#)].
- [9] LUX collaboration, D. S. Akerib et al., *Constraints on effective field theory couplings using 311.2 days of LUX data*, *Phys. Rev. D* **104** (2021) 062005, [[2102.06998](#)].
- [10] LUX collaboration, D. S. Akerib et al., *Effective field theory analysis of the first LUX dark matter search*, *Phys. Rev. D* **103** (2021) 122005, [[2003.11141](#)].
- [11] ICECUBE collaboration, R. Abbasi et al., *Constraining non-standard Dark Matter-Nucleon Interactions with IceCube*, *PoS ICRC2021* (2021) 522, [[2108.05203](#)].
- [12] N. Isgur and M. B. Wise, *Weak Decays of Heavy Mesons in the Static Quark Approximation*, *Phys. Lett. B* **232** (1989) 113–117.
- [13] W. E. Caswell and G. P. Lepage, *Effective Lagrangians for Bound State Problems in QED, QCD, and Other Field Theories*, *Phys. Lett. B* **167** (1986) 437–442.
- [14] E. Eichten and B. R. Hill, *An Effective Field Theory for the Calculation of Matrix Elements Involving Heavy Quarks*, *Phys. Lett.* **B234** (1990) 511.
- [15] R. J. Hill and M. P. Solon, *Universal behavior in the scattering of heavy, weakly interacting dark matter on nuclear targets*, *Phys.Lett.* **B707** (2012) 539–545, [[1111.0016](#)].
- [16] R. J. Hill and M. P. Solon, *WIMP-nucleon scattering with heavy WIMP effective theory*, *Phys. Rev. Lett.* **112** (2014) 211602, [[1309.4092](#)].
- [17] R. J. Hill and M. P. Solon, *Standard Model anatomy of WIMP dark matter direct detection I: weak-scale matching*, *Phys.Rev.* **D91** (2015) 043504, [[1401.3339](#)].
- [18] C.-Y. Chen, R. J. Hill, M. P. Solon and A. M. Wijangco, *Power Corrections to the Universal Heavy WIMP-Nucleon Cross Section*, *Phys. Lett.* **B781** (2018) 473–479, [[1801.08551](#)].
- [19] Q. Chen and R. J. Hill, *Direct detection rate of heavy Higgsino-like and Wino-like dark matter*, *Phys. Lett. B* **804** (2020) 135364, [[1912.07795](#)].
- [20] R. J. Hill and M. P. Solon, *Standard Model anatomy of WIMP dark matter direct detection II: QCD analysis and hadronic matrix elements*, *Phys.Rev.* **D91** (2015) 043505, [[1409.8290](#)].
- [21] A. Berlin, D. S. Robertson, M. P. Solon and K. M. Zurek, *Bino variations: Effective field theory methods for dark matter direct detection*, *Phys. Rev.* **D93** (2016) 095008, [[1511.05964](#)].
- [22] T. R. Slatyer, *Les Houches Lectures on Indirect Detection of Dark Matter*, in *Les Houches summer school on Dark Matter*, 9, 2021. [2109.02696](#).
- [23] V. Silveira and A. Zee, *SCALAR PHANTOMS*, *Phys. Lett. B* **161** (1985) 136–140.
- [24] G. Arcadi, A. Djouadi and M. Raidal, *Dark Matter through the Higgs portal*, *Phys. Rept.* **842** (2020) 1–180, [[1903.03616](#)].
- [25] A. Mitridate, M. Redi, J. Smirnov and A. Strumia, *Cosmological Implications of Dark Matter Bound States*, *JCAP* **05** (2017) 006, [[1702.01141](#)].

- [26] M. Baumgart, N. Rodd, T. Slatyer and V. Vaidya, *Siege Engines Take On Minimal Dark Matter*, **22xx.xxxxx**.
- [27] P. Ciafaloni and D. Comelli, *Sudakov enhancement of electroweak corrections*, *Phys. Lett. B* **446** (1999) 278–284, [[hep-ph/9809321](#)].
- [28] P. Ciafaloni and D. Comelli, *Electroweak Sudakov form-factors and nonfactorizable soft QED effects at NLC energies*, *Phys. Lett. B* **476** (2000) 49–57, [[hep-ph/9910278](#)].
- [29] M. Ciafaloni, P. Ciafaloni and D. Comelli, *Bloch-Nordsieck violating electroweak corrections to inclusive TeV scale hard processes*, *Phys. Rev. Lett.* **84** (2000) 4810–4813, [[hep-ph/0001142](#)].
- [30] C. W. Bauer, S. Fleming and M. E. Luke, *Summing Sudakov logarithms in  $B \rightarrow X(s\gamma)$  in effective field theory*, *Phys. Rev. D* **63** (2000) 014006, [[hep-ph/0005275](#)].
- [31] C. W. Bauer, S. Fleming, D. Pirjol and I. W. Stewart, *An Effective field theory for collinear and soft gluons: Heavy to light decays*, *Phys. Rev. D* **63** (2001) 114020, [[hep-ph/0011336](#)].
- [32] C. W. Bauer and I. W. Stewart, *Invariant operators in collinear effective theory*, *Phys. Lett. B* **516** (2001) 134–142, [[hep-ph/0107001](#)].
- [33] C. W. Bauer, D. Pirjol and I. W. Stewart, *Soft collinear factorization in effective field theory*, *Phys. Rev. D* **65** (2002) 054022, [[hep-ph/0109045](#)].
- [34] M. Baumgart, I. Z. Rothstein and V. Vaidya, *Calculating the Annihilation Rate of Weakly Interacting Massive Particles*, *Phys. Rev. Lett.* **114** (2015) 211301, [[1409.4415](#)].
- [35] M. Bauer, T. Cohen, R. J. Hill and M. P. Solon, *Soft Collinear Effective Theory for Heavy WIMP Annihilation*, *JHEP* **01** (2015) 099, [[1409.7392](#)].
- [36] G. Ovanessian, T. R. Slatyer and I. W. Stewart, *Heavy Dark Matter Annihilation from Effective Field Theory*, *Phys. Rev. Lett.* **114** (2015) 211302, [[1409.8294](#)].
- [37] M. Baumgart, I. Z. Rothstein and V. Vaidya, *Constraints on Galactic Wino Densities from Gamma Ray Lines*, *JHEP* **04** (2015) 106, [[1412.8698](#)].
- [38] M. Baumgart, T. Cohen, I. Mould, N. L. Rodd, T. R. Slatyer, M. P. Solon et al., *Resummed Photon Spectra for WIMP Annihilation*, *JHEP* **03** (2018) 117, [[1712.07656](#)].
- [39] M. Baumgart and V. Vaidya, *Semi-inclusive wino and higgsino annihilation to  $LL'$* , *JHEP* **03** (2016) 213, [[1510.02470](#)].
- [40] M. Beneke, C. Hasner, K. Urban and M. Vollmann, *Precise yield of high-energy photons from Higgsino dark matter annihilation*, *JHEP* **03** (2020) 030, [[1912.02034](#)].
- [41] MAGIC collaboration, J. Flix Molina, *Planned dark matter searches with the MAGIC Telescope*, in *40th Rencontres de Moriond on Very High Energy Phenomena in the Universe*, pp. 421–424, 2005. [[astro-ph/0505313](#)].
- [42] MAGIC, FERMI-LAT collaboration, M. L. Ahnen et al., *Limits to Dark Matter Annihilation Cross-Section from a Combined Analysis of MAGIC and Fermi-LAT Observations of Dwarf Satellite Galaxies*, *JCAP* **02** (2016) 039, [[1601.06590](#)].
- [43] T. C. Weekes et al., *VERITAS: The Very energetic radiation imaging telescope array system*, *Astropart. Phys.* **17** (2002) 221–243, [[astro-ph/0108478](#)].

- [44] VERITAS collaboration, J. Holder et al., *The first VERITAS telescope*, *Astropart. Phys.* **25** (2006) 391–401, [[astro-ph/0604119](#)].
- [45] VERITAS collaboration, A. Geringer-Sameth, *The VERITAS Dark Matter Program*, in *4th International Fermi Symposium*, 3, 2013. [1303.1406](#).
- [46] H.E.S.S. collaboration, J. A. Hinton, *The Status of the H.E.S.S. project*, *New Astron. Rev.* **48** (2004) 331–337, [[astro-ph/0403052](#)].
- [47] H.E.S.S. collaboration, A. Abramowski et al., *Search for Photon-Linelike Signatures from Dark Matter Annihilations with H.E.S.S.*, *Phys. Rev. Lett.* **110** (2013) 041301, [[1301.1173](#)].
- [48] A. Hryczuk, K. Jodkowski, E. Moulin, L. Rinchiuso, L. Roszkowski, E. M. Sessolo et al., *Testing dark matter with Cherenkov light - prospects of H.E.S.S. and CTA for exploring minimal supersymmetry*, *JHEP* **10** (2019) 043, [[1905.00315](#)].
- [49] CTA CONSORTIUM collaboration, M. Actis et al., *Design concepts for the Cherenkov Telescope Array CTA: An advanced facility for ground-based high-energy gamma-ray astronomy*, *Exper. Astron.* **32** (2011) 193–316, [[1008.3703](#)].
- [50] H. Silverwood, C. Weniger, P. Scott and G. Bertone, *A realistic assessment of the CTA sensitivity to dark matter annihilation*, *JCAP* **03** (2015) 055, [[1408.4131](#)].
- [51] V. Lefranc, E. Moulin, P. Panci and J. Silk, *Prospects for Annihilating Dark Matter in the inner Galactic halo by the Cherenkov Telescope Array*, *Phys. Rev. D* **91** (2015) 122003, [[1502.05064](#)].
- [52] M. Cirelli, G. Corcella, A. Hektor, G. Hutsi, M. Kadastik, P. Panci et al., *PPPC 4 DM ID: A Poor Particle Physicist Cookbook for Dark Matter Indirect Detection*, *JCAP* **03** (2011) 051, [[1012.4515](#)].
- [53] C. W. Bauer, N. L. Rodd and B. R. Webber, *Dark matter spectra from the electroweak to the Planck scale*, *JHEP* **06** (2021) 121, [[2007.15001](#)].
- [54] M. Beneke, A. Broggio, C. Hasner and M. Vollmann, *Energetic  $\gamma$ -rays from TeV scale dark matter annihilation resummed*, *Phys. Lett. B* **786** (2018) 347–354, [[1805.07367](#)].
- [55] M. Beneke, A. Broggio, C. Hasner, K. Urban and M. Vollmann, *Resummed photon spectrum from dark matter annihilation for intermediate and narrow energy resolution*, *JHEP* **08** (2019) 103, [[1903.08702](#)].
- [56] M. Beneke, K. Urban and M. Vollmann, *Matching resummed endpoint and continuum  $\gamma$ -ray spectra from dark-matter annihilation*, [2203.01692](#).
- [57] J. Hisano, S. Matsumoto and M. M. Nojiri, *Explosive dark matter annihilation*, *Phys. Rev. Lett.* **92** (2004) 031303, [[hep-ph/0307216](#)].
- [58] J. Hisano, S. Matsumoto, M. M. Nojiri and O. Saito, *Non-perturbative effect on dark matter annihilation and gamma ray signature from galactic center*, *Phys. Rev. D* **71** (2005) 063528, [[hep-ph/0412403](#)].
- [59] J. Hisano, S. Matsumoto, M. Nagai, O. Saito and M. Senami, *Non-perturbative effect on thermal relic abundance of dark matter*, *Phys. Lett. B* **646** (2007) 34–38, [[hep-ph/0610249](#)].
- [60] M. Beneke, C. Hellmann and P. Ruiz-Femenia, *Non-relativistic pair annihilation of nearly*



- mass degenerate neutralinos and charginos I. General framework and S-wave annihilation, *JHEP* **03** (2013) 148, [[1210.7928](#)].
- [61] C. Hellmann and P. Ruiz-Femenía, *Non-relativistic pair annihilation of nearly mass degenerate neutralinos and charginos II. P-wave and next-to-next-to-leading order S-wave coefficients*, *JHEP* **08** (2013) 084, [[1303.0200](#)].
- [62] M. Beneke, C. Hellmann and P. Ruiz-Femenia, *Non-relativistic pair annihilation of nearly mass degenerate neutralinos and charginos III. Computation of the Sommerfeld enhancements*, *JHEP* **05** (2015) 115, [[1411.6924](#)].
- [63] A. Pineda and J. Soto, *Effective field theory for ultrasoft momenta in NRQCD and NRQED*, *Nucl. Phys. B Proc. Suppl.* **64** (1998) 428–432, [[hep-ph/9707481](#)].
- [64] M. Beneke, *New results on heavy quarks near threshold*, in *3rd Workshop on Continuous Advances in QCD (QCD 98)*, pp. 293–309, 6, 1998. [hep-ph/9806429](#).
- [65] N. Brambilla, A. Pineda, J. Soto and A. Vairo, *Potential NRQCD: An Effective theory for heavy quarkonium*, *Nucl. Phys. B* **566** (2000) 275, [[hep-ph/9907240](#)].
- [66] T. R. Slatyer, *The Sommerfeld enhancement for dark matter with an excited state*, *JCAP* **02** (2010) 028, [[0910.5713](#)].
- [67] M. Beneke, R. Szafron and K. Urban, *Wino potential and Sommerfeld effect at NLO*, *Phys. Lett. B* **800** (2020) 135112, [[1909.04584](#)].
- [68] M. Beneke, R. Szafron and K. Urban, *Sommerfeld-corrected relic abundance of wino dark matter with NLO electroweak potentials*, *JHEP* **02** (2021) 020, [[2009.00640](#)].
- [69] K. Urban, *NLO electroweak potentials for minimal dark matter and beyond*, *JHEP* **10** (2021) 136, [[2108.07285](#)].
- [70] G. Ovanessian, N. L. Rodd, T. R. Slatyer and I. W. Stewart, *One-loop correction to heavy dark matter annihilation*, *Phys. Rev. D* **95** (2017) 055001, [[1612.04814](#)].
- [71] J. Bagnasco, M. Dine and S. D. Thomas, *Detecting technibaryon dark matter*, *Phys. Lett. B* **320** (1994) 99–104, [[hep-ph/9310290](#)].
- [72] M. Pospelov and T. ter Veldhuis, *Direct and indirect limits on the electromagnetic form-factors of WIMPs*, *Phys. Lett. B* **480** (2000) 181–186, [[hep-ph/0003010](#)].
- [73] A. Kurylov and M. Kamionkowski, *Generalized analysis of weakly interacting massive particle searches*, *Phys. Rev. D* **69** (2004) 063503, [[hep-ph/0307185](#)].
- [74] J. Kopp, T. Schwetz and J. Zupan, *Global interpretation of direct Dark Matter searches after CDMS-II results*, *JCAP* **1002** (2010) 014, [[0912.4264](#)].
- [75] J. Fan, M. Reece and L.-T. Wang, *Non-relativistic effective theory of dark matter direct detection*, *JCAP* **1011** (2010) 042, [[1008.1591](#)].
- [76] V. Cirigliano, M. L. Graesser and G. Ovanessian, *WIMP-nucleus scattering in chiral effective theory*, *JHEP* **10** (2012) 025, [[1205.2695](#)].
- [77] A. L. Fitzpatrick, W. Haxton, E. Katz, N. Lubbers and Y. Xu, *The Effective Field Theory of Dark Matter Direct Detection*, *JCAP* **1302** (2013) 004, [[1203.3542](#)].

- [78] A. L. Fitzpatrick, W. Haxton, E. Katz, N. Lubbers and Y. Xu, *Model Independent Direct Detection Analyses*, [1211.2818](#).
- [79] J. Menendez, D. Gazit and A. Schwenk, *Spin-dependent WIMP scattering off nuclei*, *Phys. Rev. D* **86** (2012) 103511, [[1208.1094](#)].
- [80] N. Anand, A. L. Fitzpatrick and W. C. Haxton, *Weakly interacting massive particle-nucleus elastic scattering response*, *Phys. Rev. C* **89** (2014) 065501, [[1308.6288](#)].
- [81] P. Klos, J. Menéndez, D. Gazit and A. Schwenk, *Large-scale nuclear structure calculations for spin-dependent WIMP scattering with chiral effective field theory currents*, *Phys. Rev. D* **88** (2013) 083516, [[1304.7684](#)].
- [82] M. Cirelli, E. Del Nobile and P. Panci, *Tools for model-independent bounds in direct dark matter searches*, *JCAP* **1310** (2013) 019, [[1307.5955](#)].
- [83] G. Barello, S. Chang and C. A. Newby, *A Model Independent Approach to Inelastic Dark Matter Scattering*, *Phys. Rev. D* **90** (2014) 094027, [[1409.0536](#)].
- [84] R. Catena and P. Gondolo, *Global fits of the dark matter-nucleon effective interactions*, *JCAP* **1409** (2014) 045, [[1405.2637](#)].
- [85] M. Hoferichter, P. Klos and A. Schwenk, *Chiral power counting of one- and two-body currents in direct detection of dark matter*, *Phys. Lett. B* **746** (2015) 410–416, [[1503.04811](#)].
- [86] M. Hoferichter, P. Klos, J. Menendez and A. Schwenk, *Analysis strategies for general spin-independent WIMP-nucleus scattering*, *Phys. Rev. D* **94** (2016) 063505, [[1605.08043](#)].
- [87] F. Bishara, J. Brod, B. Grinstein and J. Zupan, *Chiral Effective Theory of Dark Matter Direct Detection*, *JCAP* **1702** (2017) 009, [[1611.00368](#)].
- [88] F. Bishara, J. Brod, B. Grinstein and J. Zupan, *From quarks to nucleons in dark matter direct detection*, *JHEP* **11** (2017) 059, [[1707.06998](#)].
- [89] F. D’Eramo, B. J. Kavanagh and P. Panci, *You can hide but you have to run: direct detection with vector mediators*, *JHEP* **08** (2016) 111, [[1605.04917](#)].
- [90] F. Bishara, J. Brod, B. Grinstein and J. Zupan, *DirectDM: a tool for dark matter direct detection*, [1708.02678](#).
- [91] F. D’Eramo, B. J. Kavanagh and P. Panci, *Probing Leptophilic Dark Sectors with Hadronic Processes*, *Phys. Lett. B* **771** (2017) 339–348, [[1702.00016](#)].
- [92] J. Brod, B. Grinstein, E. Stamou and J. Zupan, *Weak mixing below the weak scale in dark-matter direct detection*, *JHEP* **02** (2018) 174, [[1801.04240](#)].
- [93] J. Brod, A. Gootjes-Dreesbach, M. Tamaro and J. Zupan, *Effective Field Theory for Dark Matter Direct Detection up to Dimension Seven*, [1710.10218](#).
- [94] M. Hoferichter, J. Menendez and A. Schwenk, *Coherent elastic neutrino-nucleus scattering: EFT analysis and nuclear responses*, [2007.08529](#).
- [95] M. Hoferichter, P. Klos, J. Menendez and A. Schwenk, *Nuclear structure factors for general spin-independent WIMP-nucleus scattering*, *Phys. Rev. D* **99** (2019) 055031, [[1812.05617](#)].
- [96] J. Aebischer, W. Altmannshofer, E. E. Jenkins and A. V. Manohar, *Dark Matter Effective Field Theory and an Application to Vector Dark Matter*, [2202.06968](#).

- [97] J. Brod, *Dark matter effective theory*, *SciPost Phys. Lect. Notes* **38** (2022) 1, [2108.11931].
- [98] S. Weinberg, *Nuclear forces from chiral Lagrangians*, *Phys. Lett.* **B251** (1990) 288–292.
- [99] S. Weinberg, *Effective chiral Lagrangians for nucleon - pion interactions and nuclear forces*, *Nucl. Phys.* **B363** (1991) 3–18.
- [100] F. Bishara, J. Brod, B. Grinstein and J. Zupan, *Renormalization Group Effects in Dark Matter Interactions*, *JHEP* **03** (2020) 089, [1809.03506].
- [101] V. Cirigliano, M. L. Graesser, G. Ovanessian and I. M. Shoemaker, *Shining LUX on Isospin-Violating Dark Matter Beyond Leading Order*, *Phys. Lett. B* **739** (2014) 293–301, [1311.5886].
- [102] M. Hoferichter, P. Klos, J. Menendez and A. Schwenk, *Dark-matter-nucleus scattering in chiral effective field theory*, *PoS CD2018* (2019) 095, [1903.11075].
- [103] LHC DARK MATTER WORKING GROUP collaboration, T. Abe et al., *LHC Dark Matter Working Group: Next-generation spin-0 dark matter models*, *Phys. Dark Univ.* **27** (2020) 100351, [1810.09420].
- [104] T. Alanne, F. Bishara, J. Fiaschi, O. Fischer, M. Gorbahn and U. Moldanazarova, *Z'-mediated Majorana dark matter: suppressed direct-detection rate and complementarity of LHC searches*, 2202.02292.
- [105] PANDAX-II collaboration, J. Xia et al., *PandaX-II Constraints on Spin-Dependent WIMP-Nucleon Effective Interactions*, *Phys. Lett. B* **792** (2019) 193–198, [1807.01936].
- [106] Z. Liu, Y. Su, Y.-L. Sming Tsai, B. Yu and Q. Yuan, *A combined analysis of PandaX, LUX, and XENON1T experiments within the framework of dark matter effective theory*, *JHEP* **11** (2017) 024, [1708.04630].
- [107] SUPERCDMS collaboration, K. Schneck et al., *Dark matter effective field theory scattering in direct detection experiments*, *Phys. Rev. D* **91** (2015) 092004, [1503.03379].
- [108] COSINE-100, SOGANG PHENOMENOLOGY GROUP collaboration, G. Adhikari et al., *COSINE-100 and DAMA/LIBRA-phase2 in WIMP effective models*, *JCAP* **06** (2019) 048, [1904.00128].
- [109] DARKSIDE-50 collaboration, P. Agnes et al., *Effective field theory interactions for liquid argon target in DarkSide-50 experiment*, *Phys. Rev. D* **101** (2020) 062002, [2002.07794].
- [110] DEAP collaboration, P. Adhikari et al., *Constraints on dark matter-nucleon effective couplings in the presence of kinematically distinct halo substructures using the DEAP-3600 detector*, 2005.14667.
- [111] CDEX collaboration, Y. Wang et al., *First Experimental Constraints on WIMP Couplings in Effective Field Theory Framework from the CDEX Experiment*, 2007.15555.
- [112] A. Crivellin, F. D’Eramo and M. Procura, *New Constraints on Dark Matter Effective Theories from Standard Model Loops*, *Phys. Rev. Lett.* **112** (2014) 191304, [1402.1173].
- [113] F. D’Eramo and M. Procura, *Connecting Dark Matter UV Complete Models to Direct Detection Rates via Effective Field Theory*, *JHEP* **04** (2015) 054, [1411.3342].
- [114] Y. Kahn and T. Lin, *Searches for light dark matter using condensed matter systems*, 2108.03239.

- [115] A. Caputo, A. Esposito and A. D. Polosa, *Sub-MeV Dark Matter and the Goldstone Modes of Superfluid Helium*, *Phys. Rev. D* **100** (2019) 116007, [[1907.10635](#)].
- [116] A. Caputo, A. Esposito, E. Geoffray, A. D. Polosa and S. Sun, *Dark Matter, Dark Photon and Superfluid He-4 from Effective Field Theory*, *Phys. Lett. B* **802** (2020) 135258, [[1911.04511](#)].
- [117] R. Catena, T. Emken, N. A. Spaldin and W. Tarantino, *Atomic responses to general dark matter-electron interactions*, *Phys. Rev. Res.* **2** (2020) 033195, [[1912.08204](#)].
- [118] T. Trickle, Z. Zhang and K. M. Zurek, *Effective field theory of dark matter direct detection with collective excitations*, *Phys. Rev. D* **105** (2022) 015001, [[2009.13534](#)].
- [119] R. Catena, T. Emken, M. Matas, N. A. Spaldin and E. Urdshals, *Crystal responses to general dark matter-electron interactions*, *Phys. Rev. Res.* **3** (2021) 033149, [[2105.02233](#)].
- [120] A. Mitridate, T. Trickle, Z. Zhang and K. M. Zurek, *Dark matter absorption via electronic excitations*, *JHEP* **09** (2021) 123, [[2106.12586](#)].
- [121] S. Knapen, T. Lin, M. Pyle and K. M. Zurek, *Detection of Light Dark Matter With Optical Phonons in Polar Materials*, *Phys. Lett. B* **785** (2018) 386–390, [[1712.06598](#)].
- [122] S. Griffin, S. Knapen, T. Lin and K. M. Zurek, *Directional Detection of Light Dark Matter with Polar Materials*, *Phys. Rev. D* **98** (2018) 115034, [[1807.10291](#)].
- [123] T. Trickle, Z. Zhang, K. M. Zurek, K. Inzani and S. M. Griffin, *Multi-Channel Direct Detection of Light Dark Matter: Theoretical Framework*, *JHEP* **03** (2020) 036, [[1910.08092](#)].
- [124] S. M. Griffin, K. Inzani, T. Trickle, Z. Zhang and K. M. Zurek, *Multichannel direct detection of light dark matter: Target comparison*, *Phys. Rev. D* **101** (2020) 055004, [[1910.10716](#)].
- [125] T. Trickle, Z. Zhang and K. M. Zurek, *Detecting Light Dark Matter with Magnons*, *Phys. Rev. Lett.* **124** (2020) 201801, [[1905.13744](#)].
- [126] T. Trickle, Z. Zhang and K. M. Zurek.
- [127] C. Chang et al., “Snowmass 2021 Letter of Interest: The TESSARACT Dark Matter Project.” 2020.
- [128] M. T. Frandsen, F. Kahlhoefer, S. Sarkar and K. Schmidt-Hoberg, *Direct detection of dark matter in models with a light  $Z'$* , *JHEP* **09** (2011) 128, [[1107.2118](#)].
- [129] P. Agrawal, S. Blanchet, Z. Chacko and C. Kilic, *Flavored Dark Matter, and Its Implications for Direct Detection and Colliders*, *Phys. Rev. D* **86** (2012) 055002, [[1109.3516](#)].
- [130] P. Agrawal, Z. Chacko, C. Kilic and R. K. Mishra, *A Classification of Dark Matter Candidates with Primarily Spin-Dependent Interactions with Matter*, [1003.1912](#).
- [131] J. Goodman and W. Shepherd, *LHC Bounds on UV-Complete Models of Dark Matter*, [1111.2359](#).
- [132] H. An, X. Ji and L.-T. Wang, *Light Dark Matter and  $Z'$  Dark Force at Colliders*, *JHEP* **07** (2012) 182, [[1202.2894](#)].
- [133] M. T. Frandsen, F. Kahlhoefer, A. Preston, S. Sarkar and K. Schmidt-Hoberg, *LHC and Tevatron Bounds on the Dark Matter Direct Detection Cross-Section for Vector Mediators*, *JHEP* **07** (2012) 123, [[1204.3839](#)].

- [134] M. Garny, A. Ibarra, M. Pato and S. Vogl, *Closing in on mass-degenerate dark matter scenarios with antiprotons and direct detection*, *JCAP* **11** (2012) 017, [[1207.1431](#)].
- [135] N. F. Bell, J. B. Dent, A. J. Galea, T. D. Jacques, L. M. Krauss and T. J. Weiler, *Searching for Dark Matter at the LHC with a Mono-Z*, *Phys. Rev. D* **86** (2012) 096011, [[1209.0231](#)].
- [136] H. An, R. Huo and L.-T. Wang, *Searching for Low Mass Dark Portal at the LHC*, *Phys. Dark Univ.* **2** (2013) 50–57, [[1212.2221](#)].
- [137] S. Chang, R. Edezhath, J. Hutchinson and M. Luty, *Effective WIMPs*, *Phys. Rev. D* **89** (2014) 015011, [[1307.8120](#)].
- [138] H. An, L.-T. Wang and H. Zhang, *Dark matter with  $t$ -channel mediator: a simple step beyond contact interaction*, *Phys. Rev. D* **89** (2014) 115014, [[1308.0592](#)].
- [139] Y. Bai and J. Berger, *Fermion Portal Dark Matter*, *JHEP* **11** (2013) 171, [[1308.0612](#)].
- [140] A. DiFranzo, K. I. Nagao, A. Rajaraman and T. M. P. Tait, *Simplified Models for Dark Matter Interacting with Quarks*, *JHEP* **11** (2013) 014, [[1308.2679](#)].
- [141] A. Alves, S. Profumo and F. S. Queiroz, *The dark  $Z'$  portal: direct, indirect and collider searches*, *JHEP* **04** (2014) 063, [[1312.5281](#)].
- [142] G. Arcadi, Y. Mambrini, M. H. G. Tytgat and B. Zaldivar, *Invisible  $Z'$  and dark matter: LHC vs LUX constraints*, *JHEP* **03** (2014) 134, [[1401.0221](#)].
- [143] Y. Bai and J. Berger, *Lepton Portal Dark Matter*, *JHEP* **08** (2014) 153, [[1402.6696](#)].
- [144] O. Lebedev and Y. Mambrini, *Axial dark matter: The case for an invisible  $Z'$ ?*, *Phys. Lett. B* **734** (2014) 350–353, [[1403.4837](#)].
- [145] J. Abdallah et al., *Simplified Models for Dark Matter and Missing Energy Searches at the LHC*, [1409.2893](#).
- [146] M. R. Buckley, D. Feld and D. Goncalves, *Scalar Simplified Models for Dark Matter*, *Phys. Rev. D* **91** (2015) 015017, [[1410.6497](#)].
- [147] A. Alves, A. Berlin, S. Profumo and F. S. Queiroz, *Dark Matter Complementarity and the  $Z'$  Portal*, *Phys. Rev. D* **92** (2015) 083004, [[1501.03490](#)].
- [148] A. Berlin, S. Gori, T. Lin and L.-T. Wang, *Pseudoscalar Portal Dark Matter*, *Phys. Rev. D* **92** (2015) 015005, [[1502.06000](#)].
- [149] A. Ismail, W.-Y. Keung, K.-H. Tsao and J. Unwin, *Axial vector  $Z'$  and anomaly cancellation*, *Nucl. Phys. B* **918** (2017) 220–244, [[1609.02188](#)].
- [150] A. Alves, G. Arcadi, Y. Mambrini, S. Profumo and F. S. Queiroz, *Augury of darkness: the low-mass dark  $Z'$  portal*, *JHEP* **04** (2017) 164, [[1612.07282](#)].
- [151] G. Arcadi, P. Ghosh, Y. Mambrini, M. Pierre and F. S. Queiroz,  *$Z'$  portal to Chern-Simons Dark Matter*, *JCAP* **11** (2017) 020, [[1706.04198](#)].
- [152] J. A. Evans, S. Gori and J. Shelton, *Looking for the WIMP Next Door*, *JHEP* **02** (2018) 100, [[1712.03974](#)].
- [153] T. Alanne and F. Goertz, *Extended Dark Matter EFT*, *Eur. Phys. J. C* **80** (2020) 446, [[1712.07626](#)].

- [154] T. Alanne, G. Arcadi, F. Goertz, V. Tenorth and S. Vogl, *Model-independent constraints with extended dark matter EFT*, *JHEP* **10** (2020) 172, [[2006.07174](#)].
- [155] S. Argyropoulos and U. Haisch, *Benchmarking LHC searches for light 2HDM+a pseudoscalars*, [2202.12631](#).
- [156] J. Abdallah et al., *Simplified Models for Dark Matter Searches at the LHC*, *Phys. Dark Univ.* **9-10** (2015) 8–23, [[1506.03116](#)].
- [157] A. Boveia et al., *Recommendations on presenting LHC searches for missing transverse energy signals using simplified s-channel models of dark matter*, *Phys. Dark Univ.* **27** (2020) 100365, [[1603.04156](#)].
- [158] D. Abercrombie et al., *Dark Matter benchmark models for early LHC Run-2 Searches: Report of the ATLAS/CMS Dark Matter Forum*, *Phys. Dark Univ.* **27** (2020) 100371, [[1507.00966](#)].
- [159] A. Albert et al., *Towards the next generation of simplified Dark Matter models*, *Phys. Dark Univ.* **16** (2017) 49–70, [[1607.06680](#)].
- [160] A. Albert et al., *Recommendations of the LHC Dark Matter Working Group: Comparing LHC searches for dark matter mediators in visible and invisible decay channels and calculations of the thermal relic density*, *Phys. Dark Univ.* **26** (2019) 100377, [[1703.05703](#)].
- [161] S. Tulin and H.-B. Yu, *Dark Matter Self-interactions and Small Scale Structure*, *Phys. Rept.* **730** (2018) 1–57, [[1705.02358](#)].
- [162] N. Arkani-Hamed, D. P. Finkbeiner, T. R. Slatyer and N. Weiner, *A Theory of Dark Matter*, *Phys. Rev. D* **79** (2009) 015014, [[0810.0713](#)].
- [163] M. Pospelov and A. Ritz, *Astrophysical Signatures of Secluded Dark Matter*, *Phys. Lett. B* **671** (2009) 391–397, [[0810.1502](#)].
- [164] M. R. Buckley and P. J. Fox, *Dark Matter Self-Interactions and Light Force Carriers*, *Phys. Rev. D* **81** (2010) 083522, [[0911.3898](#)].
- [165] J. L. Feng, M. Kaplinghat and H.-B. Yu, *Halo Shape and Relic Density Exclusions of Sommerfeld-Enhanced Dark Matter Explanations of Cosmic Ray Excesses*, *Phys. Rev. Lett.* **104** (2010) 151301, [[0911.0422](#)].
- [166] A. Loeb and N. Weiner, *Cores in Dwarf Galaxies from Dark Matter with a Yukawa Potential*, *Phys. Rev. Lett.* **106** (2011) 171302, [[1011.6374](#)].
- [167] S. Tulin, H.-B. Yu and K. M. Zurek, *Beyond Collisionless Dark Matter: Particle Physics Dynamics for Dark Matter Halo Structure*, *Phys. Rev. D* **87** (2013) 115007, [[1302.3898](#)].
- [168] G. P. Lepage, *How to renormalize the Schrodinger equation*, in *Nuclear physics. Proceedings, 8th Jorge Andre Swieca Summer School, Sao Jose dos Campos, Campos do Jordao, Brazil, January 26-February 7, 1997*, pp. 135–180, 1997. [nucl-th/9706029](#).
- [169] B. Bellazzini, M. Cliche and P. Tanedo, *Effective theory of self-interacting dark matter*, *Phys. Rev. D* **88** (2013) 083506, [[1307.1129](#)].
- [170] B. A. Dobrescu and I. Mocioiu, *Spin-dependent macroscopic forces from new particle exchange*, *JHEP* **11** (2006) 005, [[hep-ph/0605342](#)].
- [171] P. Agrawal, A. Parikh and M. Reece, *Systematizing the Effective Theory of Self-Interacting Dark Matter*, *JHEP* **10** (2020) 191, [[2003.00021](#)].

- [172] A. Parikh, *The singularity structure of quantum-mechanical potentials*, *Phys. Rev. D* **104** (2021) 036005, [[2012.11606](#)].
- [173] F. Kahlhoefer, K. Schmidt-Hoberg and S. Wild, *Dark matter self-interactions from a general spin-0 mediator*, *JCAP* **08** (2017) 003, [[1704.02149](#)].